

# Detection of Abnormality in Endoscopic Images using Endoscopic Technique

Shrikant D.Kale

Dept of Electronics & Telecommunication  
C.O.E.T.Sipna  
Amravati, India  
*shrikantkale.amravati@gmail.com*

Dr.S.B.Kasturiwala

Asst. Prof., Dept of Electronics & Telecommunication  
C.O.E.T.Sipna  
Amravati, India  
*sanket.kasturiwala@gmail.com*

**Abstract**—Medical imaging has been undergoing a revolution in the past decade with the advent of faster, more accurate and less invasive devices. This has driven the need for corresponding software development which in turn has provided a major impetus for new algorithms in signal and image processing. Digital image processing is important for many biomedical applications. The medical images analyzed, used as diagnostic tools and quite often provide insight into the inner working of the process under study. The commonly found abnormalities in endoscopic images are cancer tumors, ulcers, bleeding due to internal injuries, etc. The segmented method is used to segment the tumor, abnormal regions and cancerous growth in the human esophagus. In our proposed work, a method for detecting possible presence of abnormality in the endoscopic images is presented. An algorithm is developed to perform the segmentation, classification and analysis of medical images, especially the endoscopic images for the identification of commonly occurring abnormalities in it.

**Keywords**-*medical; abnormality; endoscopic image; segmentation; esophagus; biomedical applications*

\*\*\*\*\*

## I. INTRODUCTION

An endoscope is one of the most important inventions in the history of gastroenterology. Endoscopic examination has led physicians to understand the lesion in vivo not only by abstract imagination but by vivid images also.

Endoscopy means looking inside and typically refers to looking inside the body for medical reasons using an endoscope, an instrument used to examine the interior of a hollow organ or cavity of the body. Unlike most other medical imaging devices, endoscopes are inserted directly into the organ. There are many different types of endoscope, and depending on the site in the body and the type of procedure, endoscopy may be performed by a doctor or a surgeon, and the patient may be fully conscious or under general anesthetic. Endoscope can also refer to using a bore scope in technical situations where direct line of-sight observation is not feasible. White light image (WLI) based on all spectrum of visible ray produces natural colors and shapes that we see every day. However, it is often not enough to recognize the presence or the extent of the lesion in WLI due to obscure contrasting between the lesion and the background mucosa. Thus, engineers and endoscopists put effort to develop new technology to find out and characterize the lesions easily. Now, endoscopists can acquire diverse imaging methods based on specific spectrums of light and fluorescence, as well as visible ray.<sup>1,2</sup> Furthermore, magnifying endoscopy and confocal laser endomicroscopy brought us new perspectives which were totally different from non-magnified images and let us estimate histologic changes according to specific images.

The application of digital image processing (DIP) in endoscopic ultra-sonography (EUS) images and other imaging scenarios has been proven to be a useful adjunct to endoscopic diagnoses and often comparable with specialists interpretation in different pathologic settings. The texture parameters of EUS

images are extracted and classified from the returned echoes to identify the tissue type present in the images. The analysis of the endoscopic images performed through visually and qualitatively has many drawback such as time-consuming procedures, subjective diagnosis by the expert, interpretational variation, and non-suitability for comparative evaluation. Hence a computer-assisted scheme will help considerably in the quantitative characterization of abnormalities thereby increase in the overall efficiency in managing the patient. Computer-assisted diagnosis in endoscopy consists of endoscopic image acquisition, image processing, parametric feature extraction, and classification. A number of schemes have been proposed to develop the methods for computer-assisted diagnosis for the detection of abnormal images. The presence of abnormality such as the bleeding, growth of tumors, presence of polyps, polypoid lesions and cancerous growth will lead to the presence of rough surface in the endoscopic image for which watershed segmentation will provide the better features for further analysis as compared to the simple edge analysis, since the morphological watershed segmentation embodies the basic principal concepts such as detection of discontinuity, thresholding and region processing, apart from producing more stable segmentation results, including the continuous segmentation boundaries.

## II. PROPOSED SYSTEM

The block diagram for proposed system is shown below. The proposed method is divided in main categories are as follows

- Training
- Testing



Figure 1. Block diagram of proposed work.

### A. Training

In the proposed method, the training phase of the algorithm consists only of storing the feature vectors and class labels of the training samples. The feature vectors are derived by using steps like database loading, image preprocessing, LAB color space conversion, DWT, thresholding and segmentation. For training, two classes of 8 images i.e. images of normal class and abnormal class are used which forms the vector of  $8 \times 16$ . These extracted features are stored in 'dbfeatures.mat'. These classes are supervised classes well examined and characterized by the physician. Training phase of algorithm follows the following steps.

- Load Database
- Preprocessing
- Color Space Conversion
- Wavelet Transformation
- Image Segmentation & Thresholding

### B. Testing

In the testing phase, the features of images are compared with the stored feature and the images are classified in normal and abnormal classes by using KNN classification. In the testing phase, the algorithm follows the following steps

- Load Image
- Preprocessing
- Color Space Conversion
- Wavelet Transformation
- Image Segmentation & Thresholding
- Classification

## III. IMAGE PROSESSING TECHNIQUE

### A. Adaptive Median Filter

These filters smoothes the data while keeping the small and sharp details. The median is just the middle value of all the values of the pixels in the neighborhood. Note that this is not the same as the average (or mean); instead, the median has half the values in the neighborhood larger and half smaller. The median is a stronger "central indicator" than the average. In particular, the median is hardly affected by a small number of discrepant values among the pixels in the neighborhood. Consequently, median filtering is very effective at removing various kinds of noise. The adaptive median filter also applies the noise detection and filtering algorithms to remove impulsive noise. The size of the window applied to filter the image pixels is adaptive in nature, i.e. the window size is increased if the specified condition does not meet. If the condition is met, the pixel is filtered using the median of the window. Let,  $I_{ij}$  be the pixel of the corrupted image,  $I_{\min}$  be the minimum pixel value and  $I_{\max}$  be the maximum pixel value in the window,  $W$  be the current window size applied,  $W_{\max}$  be

the maximum window size that can be reached and  $I_{\text{med}}$  be the median of the window assigned. Then, the algorithm of this filtering technique completes in two levels as described:

Level A:

a) If  $I_{\min} < I_{\text{med}} < I_{\max}$ , then the median value is not an impulse, so the a logarithm goes to Level B to check if the current pixel is an impulse.

b) Else the size of the window is increased and Level A is repeated until the median value is not an impulse so the algorithm goes to Level B; or the maximum window size is reached, in which case the median value is assigned as the filtered image pixel value.

Level B:

a) If  $I_{\min} < I_{ij} < I_{\max}$ , then the current pixel value is not an impulse, so the filtered image pixel is unchanged.

b) Else the image pixel is either equal to  $I_{\max}$  or  $I_{\min}$  (corrupted), then the filtered imaged pixel is assigned the median value from Level A.

### B. Lab Color Space

CIE  $L^*a^*b^*$  (CIELAB) is a color space specified by the International Commission on Illumination (French Commission internationale de l'éclairage, hence its CIE initialism) [18][19]. It describes all the colors visible to the human eye and was created to serve as a device-independent model to be used as a reference. The three coordinates of CIELAB represent the lightness of the color ( $L^* = 0$  yields black and  $L^* = 100$  indicates diffuse white; specular white may be higher), its position between red/magenta and green ( $a^*$ , negative values indicate green while positive values indicate magenta) and its position between yellow and blue ( $b^*$ , negative values indicate blue and positive values indicate yellow). The asterisk (\*) after  $L$ ,  $a$  and  $b$  are pronounced *star* and are part of the full name, since they represent  $L^*$ ,  $a^*$  and  $b^*$ , to distinguish them from Hunter's  $L$ ,  $a$ , and  $b$ . Since the  $L^*a^*b^*$  model is a three-dimensional model, it can be represented properly only in a three-dimensional space. Two-dimensional depictions include chromaticity diagrams: sections of the color solid with a fixed lightness. It is crucial to realize that the visual representations of the full gamut of colors in this model are never accurate; they are there just to help in understanding the concept. Because the red-green and yellow-blue opponent channels are computed as differences of lightness transformations of (putative) cone responses, CIELAB is a chromatic value color space. A related color space, the CIE 1976 ( $L^*$ ,  $u^*$ ,  $v^*$ ) color space (a.k.a. CIELUV), preserves the same  $L^*$  as  $L^*a^*b^*$  but has a different representation of the chromaticity components. CIELAB and CIELUV can also be expressed in cylindrical form (CIELCH and CIELCH<sub>uv</sub>, respectively), with the chromaticity components replaced by correlates of chrome and hue. Since CIELAB and CIELUV, the CIE has been incorporating an increasing number of color appearance phenomena into their models, to better model color vision. These color appearance models, of which CIELAB is a simple example, culminated with CIECAM02. In this color space, we have one channel is for Luminance (Lightness) and other two color channels are  $a$  and  $b$  known as chromaticity layers. The  $a^*$  layer indicates where the color falls along the red green axis, and  $b^*$  layer indicates where the color falls along the blue-yellow axis.  $a^*$  negative values indicate green while positive values indicate magenta; and  $b^*$  negative values indicate blue and positive values indicate yellow.

### C. Morphological Segmentation

The techniques that are used to find the objects of interest are usually referred to as segmentation techniques – segmenting the foreground from background. In some image analysis and machine vision applications such as industrial defect inspection or biomedical imaging segmentation based on thresholding or edge detection is not sufficient because the image quality is insufficient or the objects under inspection touch or overlap. In such applications, morphological segmentation is an effective method of image segmentation. Morphological segmentation partitions an image based on the topographic surface of the image. The image is separated into non-overlapping regions with each region containing a unique particle. Thresholding can segment objects from the background only if the objects are well separated from each other and have intensity values that differ significantly from the background. Binary morphology operators, such as close or open, often return inaccurate results when segmenting overlapping particles. Use morphological segmentation to segment touching or overlapping objects from each other and from the background. Morphology is the study of the shape and form of objects. Morphological image analysis can be used to perform Object extraction, Image filtering operations, such as removal of small objects or noise from an image, image segmentation operations such as separating connected objects and measurement operations such as texture analysis and shape description.

### D. KNN Classification

K nearest neighbors is a simple algorithm that stores all available cases and classifies new cases based on a similarity measure (e.g., distance functions). KNN has been used in statistical estimation and pattern recognition already in the beginning of 1970's as a non-parametric technique. Classification is a decision-theoretic approach to identify the image or parts of the image. Image classification is one important branch of Artificial Intelligence (AI) and most commonly used method to classify the images among the set of predefined categories by using samples of a class. Image classification was categorized into two types; they are unsupervised and supervised image classification. Since the present work is based on the techniques of supervised classification algorithms rather than unsupervised classification algorithms. Supervised classification is the most fundamental classification in machine vision classification. It requires prior knowledge of image classes. Training samples and test samples are used for classification purpose. The training examples are vectors in a multidimensional feature space, each with a class label. The training phase of the algorithm consists only of storing the feature vectors and class labels of the training samples. In the classification phase,  $k$  is a user-defined constant, and an unlabeled vector (a query or test point) is classified by assigning the label which is most frequent among the  $k$  training samples nearest to that query point.

- In  $k$ -NN classification, the output is a class membership. An object is classified by a majority vote of its neighbors, with the object being assigned to the class most common among its  $k$  nearest neighbors ( $k$  is a positive integer, typically small). If  $k = 1$ , then the object is simply assigned to the class of that single nearest neighbor.
- In  $k$ -NN regression, the output is the property value for the object. This value is the average of the values of its  $k$  nearest neighbors.

Both for classification and regression, it can be useful to assign weight to the contributions of the neighbors, so that the nearer neighbors contribute more to the average than the more distant ones. For example, a common weighting scheme consists in giving each neighbor a weight of  $1/d$ , where  $d$  is the distance to the neighbor. The neighbors are taken from a set of objects for which the class (for  $k$ NN classification) or the object property value (for  $k$ NN regression) is known. This can be thought of as the training set for the algorithm, though no explicit training step is required. A shortcoming of the  $k$ NN algorithm is that it is sensitive to the local structure of the data.

Suppose that each training class is represented by a prototype (or mean) vector:

$$m_j = 1/N_j \sum_{x \in \omega_j} x \text{ for } j = 1, 2, \dots, M$$

Where  $N_j$  is the number of training pattern vectors from class  $\omega_j$ .

## IV. ALGORITHM

With the minimum distance classifier we designed the classifier as follows. In the first, the large sequence of the image is used to find the vector for the classifier. Here in the proposed system we use 16 training sequence which are divided in to the group of two i.e. normal and abnormal. From these images the parameters are found for normal and abnormal images. So the vector  $8 \times 16$  for this sequence is found. The vector 8 defines the parameters and the vector 16 defines the number of images are used. For the classification of the images  $K$  nearest neighbors is used as it is a simple algorithm that stores all available cases and classifies new cases based on a similarity measure (e.g., distance functions). The proposed KNN classification based algorithm can be summarized in the following detail steps.

### A. Starting (Training Phase)

The training phase of the algorithm consists only of storing the feature vectors and class labels of the training samples. Two classes of 8 images i.e. normal and abnormal which form the vector  $8 \times 16$ , proceed to step B. If the training sequence is abort, proceed to step E.

### B. Process (Transformation Phase)

In the transformation phase, DWT is used for recognizing the light reflected from secreted bubbles.  $dwt2$  decomposed the images in the form of wavelet coefficient. In proposed algorithm, the decomposition of the image is to identify the brighter area, proceed to step C.

### C. Segment (Segmentation Phase)

Morphological segmentation, segments the processed image to bifurcate the light reflected area and abnormal region. The features are identified from segmented area using histogram based thresholding, proceed to step D.

### D. Classify (Classification Phase)

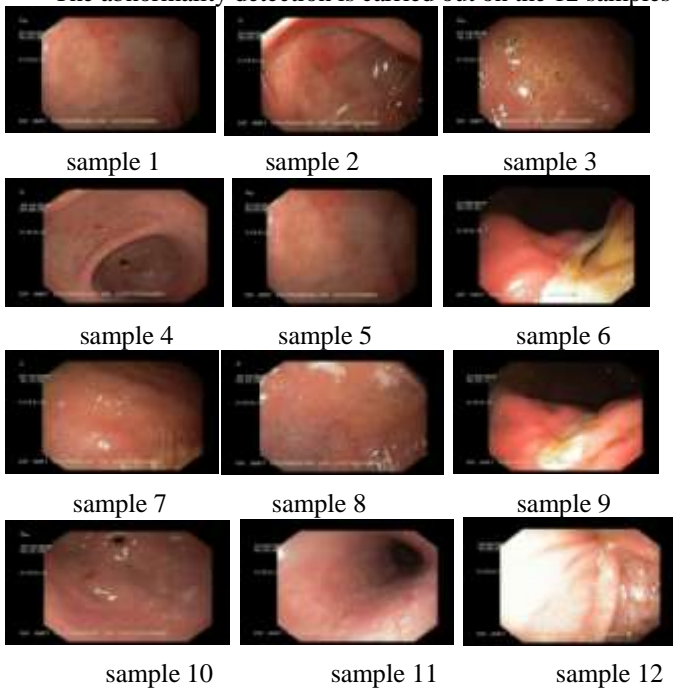
In the classification phase,  $k=2$  and an unlabeled vector (a query or test point) is classified by assigning the label which is most frequent among the  $k$  training samples nearest to that query point, proceed to step E.

### E. Ending

Bifurcate the search in two classes normal and abnormal. Depending upon the classification done in Step D, throw the message as "Abnormal" or "Normal". If the sequence of training is break, stop the process and restart again.

V. RESULT

The abnormality detection is carried out on the 12 samples



The results of normal and abnormal samples are categorized on the basis of features like area, perimeter, and number of black pixel of segmented region and area, perimeter, number of black pixel, min & max wavelet coefficient in the form of pixel for the normal and abnormal region. The following table shows the required observation

TABLE I. WAVELET ANALYSIS

Sr No	Sample	Wavelet coefficient				
		Area	Perimeter	Min coefficient	max coefficient	Form Factor
1	Sample1	18683	54.2843	0.0412	2.0000	79.6321
2	Sample2	30832	952.1320	0.0078	1.9941	0.4272
3	Sample3	28348	845.5046	0.0000	2.0000	0.5016
4	Sample4	35068	822.5685	0.0490	1.9863	0.6510
5	Sample5	28443	0.0000	0.0157	2.0000	Inf
6	Sample6	19659	967.7372	0.0078	2.0008	0.2637
7	Sample7	30409	1.111e3	0.0039	2.0000	0.3094
8	Sample8	33856	19.6569	0.0000	2.0000	1.1005e3
9	Sample9	17423	1.2590e3	0.0157	1.9922	0.1381
10	Sample10	35032	790.8112	0.0784	2.0000	0.7036
11	Sample11	19991	195.1960	0.0118	1.9922	6.5900
12	Sample12	4053	11.4142	0.4157	2.0000	390.7277

\*Inf stands for infinity

TABLE II. REGION OF INTEREST ANALYSIS

Sr No	Sample	Segmented Region				Classification 1-Normal 2-Abnormal	Physician View*
		Area	Perimeter	black pixel	Form Factor		
1	Sample1	18	31.4558	140645	0.2285	1	Normal
2	Sample2	2	2	140050	6.2800	2	Abnormal
3	Sample3	1	1	140050	6.2800	2	Abnormal
4	Sample4	45	58.4853	134328	0.1632	2	Abnormal
5	Sample5	605	120.8701	139264	0.5201	1	Normal
6	Sample6	107	37.6569	140680	0.9477	2	Abnormal
7	Sample7	49	24	141422	1.0685	2	Abnormal
8	Sample8	317	91.6985	141127	0.4735	1	Normal
9	Sample9	411	221.0366	139613	0.1057	2	Abnormal
10	Sample10	63	28	137809	1.0093	2	Abnormal
11	Sample11	71	29.4142	141475	1.0307	1	Normal
12	Sample12	56	26	141613	1.0405	1	Normal

\* the result may vary clinically or physician by physician

VI. PERFORMANCE ANALYSIS & CONCLUSION

Performance evaluation is mandatory in all automated disease recognition system and is conducted in this study to evaluate the ability of the above system for the detecting the abnormality in the endoscopic images. Accuracy of the system is found out to determine the correctness of the automatic screening of system.

Accuracy factor is defines as ratio of correctly identified results to total observations.

$$Accuracy = \frac{\text{samples correctly detected}}{\text{number of samples}} \times 100$$

$$= \frac{11}{12} \times 100 = 91.67\%$$

Total 12 samples were taken out of 11 found to be correctly identified. The accuracy of the system is 91.67%.

In the proposed work, the Haar dwt is used for extracting the foreground from background. From Table I we concluded that the form factor for wavelet transformed of normal samples is very high whereas for abnormal samples it is very low i.e. less than 1. This is because; the boundary of region interest is very large.

VII. FALSE CASE DETECTION

In the above observation the sample3 shows the random result. The sample for analysis is shown below.

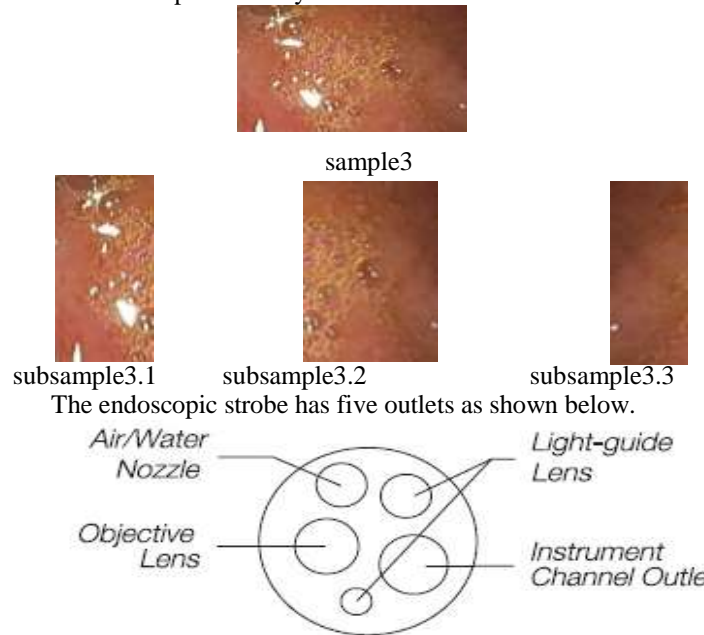


Figure 2. Front view of endoscopic strobe.

When the scope is inserted inside the body, to enlarge the cavity so that scope moves easily; the air/water is blown through the provided nozzle. The air bubbles are formed due to air/water blown and the secretion of liquid in the stomach or saliva. When the sample is divided in to three subsamples, then it is observed that

- False abnormality is detected in “subsample3.1” due to the lights reflected from the bubbles of air.
- False abnormality is detected in “subsample3.2” due to shadow of the curvature of bubbles due secretion of liquid in the stomach and saliva.

- False abnormality is detected in “subsample3.3” due to shadow at boundary of the cavity to be examined due to its adjacent organ.

#### ACKNOWLEDGMENT

The proposed work is well discussed with and well guided by and endoscopic images are provided by Dr. Amit Kavimandan.

#### REFERENCES

- [1] Shrikant D.Kale, Dr.S.B.Kasturiwala,“A Review On Detection Of Abnormality In Endoscopic Image using Image Processing Technique”, IJRCCCE, Vol - 4 , Issue - 10 October 2016.
- [2] B.V.Dhandra, Ravindra Hegadi, Mallikarjun Hangarge, V.S.Malemath,“Analysis of Abnormality in Endoscopic images using Combined HSI Color Space and Watershed Segmentation”,IEEE,pp.5243-5246,2006.
- [3] Erzhong Hu ; Nosato, H. ; Sakanashi, H. and Murakawa, M., “A modified anomaly detection method for capsule endoscopy images using nonlinear color conversion and Higher order Local AutoCorrelation (HLAC)”, Engineering in Medicine and Biology Society (EMBC), 2013 35<sup>th</sup>Annual International Conference of the IEEE, pages 5477-5480.
- [4] Erzhong Hu ; Nosato, H. ; Sakanashi, H. and Murakawa, M., “Anomaly detection for capsule endoscopy images using higherorder Local Auto Correlation features”, Systems, Man, and Cybernetics (SMC), 2012 IEEE International Conference on, pages 2289-2293.
- [5] Krishnan, S.M., Yang, X. ; Chan, K.L. and Kumar, S., “Intestinal abnormality detection from endoscopic images”, Engineering in Medicine and Biology Society, 1998. Proceedings of the 20th Annual International Conference of the IEEE (Volume:2 ), pages 895-898 vol.2
- [6] S. Allwin Devaraj, T. Kumarasamy, V. Balaji Gobi Ganesh C. Collins Christo Ranjan, A. Ganesh Narayanan, “ NORMALIZED CUTS BASED SEGMENTATION OF GASTROENTROLOGY IMAGES USING VISUAL FEATURES”, International Journal For Technological Research In Engineering Volume 1, Issue 11, July-2014
- [7] Ivanna K. Timotius, ShaouGang Miaou and YiHung Liu, “ABNORMALITY DETECTION FOR CAPSULE ENDOSCOPE IMAGES BASED ON SUPPORT VECTOR MACHINES”, Biomedical Engineering: Applications, Basis and Communications, Volume 24, Issue 01, February 2012
- [8] Thapliyal, Himanshu, and M. B. Srinivas, “Abnormality Detection in Endoscopic Images Using Color Segmentation and Curvature Computation”, Neural Information Processing Lecture, Notes in Computer Science Volume 3316, 2004, pp 834841
- [9] Baopu Li, Max Q. H. Meng, “Texture analysis for ulcer detection in capsule endoscopy images”, ELSEVIER, Image and Vision Computing 27 (2009) 1336–1342
- [10] B. V. Dhandra and Ravindra Hegadi, “Active Contours without Edges and Curvature Analysis for Endoscopic Image Classification”, International Journal of Computer Science and Security, Volume (1): Issue (1), pages 19-32
- [11] R. Kwitt, N. Vasconcelos, N. Rasiwasia, A. Uhlc, B. Davis, M. Häfner, F. Wrba, “Endoscopic image analysis in semantic space”, Medical Image Analysis 16 (2012) 1415–1422.
- [12] Philip W. Mewes, Dominik Neumann, Oleg Licegevic, Johannes Simon, Aleksandar Lj.Juloski, and Elli Angelopoulou, “Automatic Region-of-Interest Segmentation and Pathology Detection in Magnetically Guided Capsule Endoscopy”,
- [13] Deepti Shikha and B.V. Dhandra, “Abnormality detection in endoscopic images of throat cancer by morphological operations”, Indian Streams Research Journal, Vol - I, Issue - IV May 2011.
- [14] "Endoscopy". Cancer Research UK. Retrieved 5 November 2015.
- [15] Key to way stomach expands found. BBC (3 March 2008)
- [16] Sherwood, Lauralee (1997). Human physiology: from cells to systems. Belmont, CA: Wadsworth Pub. Co. ISBN 0-314-09245-5. OCLC 35270048.
- [17] Linda G. Shapiro and George C. Stockman (2001): “Computer Vision”, pp 279-325, New Jersey, Prentice-Hall, ISBN 0-13-030796-3
- [18] Barghout, Lauren, and Lawrence W. Lee. "Perceptual information processing system." Paravue Inc. U.S. Patent Application 10/618,543, filed July 11, 2003.
- [19] Hunter, Richard Sewall (July 1948). "photoelectric color-difference meter". Josa 38 (7): 661. (Proceedings of the winter meeting of the optical society of America)
- [20] Hunter, Richard Sewall (December 1948). "Accuracy, precision, and stability of new photo-electric color - difference meter". Josa 38 (12): 1094. (Proceedings of the thirty -third annual meeting of the optical society of America)
- [21] [http://en.wikipedia.org/wiki/Lab\\_color\\_space](http://en.wikipedia.org/wiki/Lab_color_space)
- [22] [http://dba.med.sc.edu/price/irf/Adobe\\_tg/models/cielab.htm](http://dba.med.sc.edu/price/irf/Adobe_tg/models/cielab.htm)